Atmos. Chem. Phys. Discuss., 15, 17317–17365, 2015
www.atmos-chem-phys-discuss.net/15/17317/2015/
doi:10.5194/acpd-15-17317-2015

Atmospheric Chemistry and Physics Discussions

Hygroscopic properties and cloud condensation nuclei activation of limonene-derived organosulfates and their mixtures with ammonium sulfate

A. M. K. Hansen[1], J. Hong[2], T. Raatikainen[3], K. Kristensen[1], A. Ylisirniö[4], A. Virtanen[4], T. Petäjä[2], M. Glasius[1], and N. L. Prisle[2]

[1]Department of Chemistry and iNANO, Aarhus University, Aarhus, Denmark
[2]Department of Physics, University of Helsinki, Helsinki, Finland
[3]Finnish Meteorological Institute, Helsinki, Finland
[4]Department of Applied Physics, University of Eastern Finland, Kuopio, Finland

Received: 13 May 2015 – Accepted: 27 May 2015 – Published: 25 June 2015

Correspondence to: N. L. Prisle (prisle@mappi.helsinki.fi)

Published by Copernicus Publications on behalf of the European Geosciences Union.

Abstract

Even though organosulfates have been observed as constituents of atmospheric aerosols in a wide range of environments spanning from the subtropics to the high Arctic, their hygroscopic properties have not been investigated prior to this study. Here, limonene-derived organosulfates with a molecular weight of 250 Da (L-OS 250) were synthesized and used for simultaneous measurements with a Hygroscopicity Tandem Differential Mobility Analyzer (H-TDMA) and a Cloud Condensation Nuclei Counter (CCNC) to determine the hygroscopicity parameter, κ, for pure L-OS 250 and mixtures of L-OS 250 with ammonium sulfate (AS) over a wide range of humidity conditions. The κ values derived from measurements with H-TDMA decreased with increasing particle dry size for all chemical compositions investigated, indicating size dependency and/or surface effects. For pure L-OS 250, κ was found to increase with increasing relative humidity, indicating dilution/solubility effects to be significant. Discrepancies in κ between the sub- and supersaturated measurements were observed for L-OS 250, whereas κ of AS and mixed L-OS 250/AS were similar. This discrepancy was primarily ascribed to limited dissolution of L-OS 250 at subsaturated conditions. In general, hygroscopic growth factor, critical activation diameter and κ for the mixed L-OS 250/AS particles converged towards the values of pure AS for mixtures with $\geq 20\,\%\,w/w$ AS. Surface tension measurements of bulk aqueous L-OS 250/AS solutions showed that L-OS 250 was indeed surface active, as expected from its molecular structure, decreasing the surface tension of solutions with 24 % from the pure water-value at a L-OS 250 concentration of $0.0025\,\mathrm{mol\,L^{-1}}$. Based on these surface tension measurements, we present the first concentration-dependent parametrisation of surface tension for aqueous L-OS 250, which was implemented to different process-level models of L-OS 250 hygroscopicity and CCN activation. The values of κ obtained from the measurements were compared with κ calculated applying the volume additive Zdanovskii–Stokes–Robinson mixing rule, as well as κ modelled from equilibrium Köhler theory with different assumptions regarding L-OS 250 bulk-to-surface partitioning and aqueous droplet

ACPD
15, 17317–17365, 2015

surface tension. This study is to our knowledge the first to investigate the hygroscopic properties and surface activity of L-OS 250; hence it is an important first step towards understanding the atmospheric impact of organosulfates.

1 Introduction

Atmospheric aerosols still account for major uncertainties in our understanding of global climate and predictions of future climate change (IPCC, 2013). In particular the indirect radiative effects of organic aerosols, i.e. their influence on cloud drop formation and cloud properties, remain insufficiently constrained for reliable model predictions of both thermodynamic and large scale general circulation levels (Hallquist et al., 2009). The intrinsic cloud condensation nuclei (CCN) activity of many organic aerosol components remain uncharacterized, just as our understanding of the various effects of mixing interactions in the aerosol phase is incomplete. Part of the uncertainty relates to the effect of organic surface activity in aqueous droplets. Surface active organic molecules (surfactants) are frequently observed in atmospheric aerosol and cloud and fog water samples (Facchini et al., 1999; Mochida et al., 2002; Cheng et al., 2004; Lin et al., 2010; Song et al., 2012) and their aqueous extracts (Dinar et al., 2006), collectively comprising a significant fraction of the organic aerosol mass. For example, Humic-Like substances (HULIS), which are surface active, have been found to account for up to 60 % of water-soluble carbon in rural aerosols (Kiss et al., 2005).

Organosulfates (organic sulfate esters) have been observed as constituents of atmospheric aerosols in a wide range of environments, such as southeastern US (Surratt et al., 2008; Lin et al., 2012), northern Europe (Iinuma et al., 2007; Froyd et al., 2010; Kristensen and Glasius, 2011; Nguyen et al., 2014) and even the Arctic, where organosulfates have been found to comprise 7–15 % of total organic matter and 9–11 % of submicron organic matter in two independent studies (Frossard et al., 2011; Hansen et al., 2014). Some organosulfates derived from monoterpenes contain a hydrophobic

ACPD
15, 17317–17365, 2015

carbon ring and are anticipated to preferably stay at the liquid/air interface in aqueous solution (i.e. exhibit surface activity); however, this has not been investigated.

Surface activity and how it is accounted for in the thermodynamic representation of aerosol water uptake has been found to significantly impact model predictions of CCN activity for some atmospheric organics (Prisle et al., 2008, 2010b). These effects have in turn been demonstrated to translate into impacts on large-scale atmospheric modelling of cloud-climate interactions and radiative forcing of comparable magnitude to the existing uncertainty in climate modelling (Prisle et al., 2012). However, to this date only a limited number of organic aerosol systems have been characterized in terms of their surface activity and the impact on cloud activation.

The hygroscopicity parameter κ (kappa) was introduced by Petters and Kreidenweis (2007) as a single variable to account for chemical effects on aerosol water uptake in equilibrium Köhler predictions of droplet growth and cloud activation. The κ-value is defined as an operational parameter and can be obtained from measurements of either hygroscopic water uptake in the sub-saturated humidity regime, or from the critical point of cloud droplet activation at supersaturated conditions, i.e. the supersaturation threshold or activation diameter. As an operationally defined parameter, the κ-value can be seen as describing aerosol–water mixing interactions with respect to a volume-based reference state. As aerosol growth is a combined effect of water uptake properties of components within the aerosol mixture, a range of aerosol–water mixing states is spanned by the subsaturated and supersaturated measurements, respectively (Prisle et al., 2010a). Provided that interactions of the mixture of individual aerosol components with water remain unchanged (or "ideal", as defined with respect to a certain reference state) over the entire concentration range spanned by measurements, the κ-value determined at different humidities, and at sub- and supersaturated conditions in particular, should remain unchanged. However, (non-ideal) mixing interactions of especially organic aerosol components with water are largely unknown and may be very complex, in particular in the presence of inorganics in the mixture (Prisle et al., 2010a). In general, previous studies comparing κ-values at sub- and supersatu-

ACPD
15, 17317–17365, 2015

rated conditions found that the subsaturated κ-values were lower than supersaturated κ-values for both ambient aerosols and laboratory-generated aerosols, especially in the case of secondary organic aerosol (Good et al., 2010; Massoli et al., 2010; Cerully et al., 2011; Dusek et al., 2011; Hersey et al., 2013; Hong et al., 2014; Pajunoja et al., 2015), however a few studies found the discrepancy to be insignificant for some aerosol compositions and particle sizes (Good et al., 2010; Dusek et al., 2011).

To our knowledge, atmospherically relevant OS have not yet been characterized in terms of their hygroscopic properties and in particular their intrinsic κ-values and effects of mixing interactions on the κ-values for particles comprising OS are not known, despite their apparent atmospheric abundance and widespread relevance. Here, we have synthesized an atmospherically relevant OS, derived from limonene with a molecular weight of 250 Da (L-OS 250), for systematic hygroscopicity characterization of this compound as a proxy for the many monoterpene-derived organosulfates observed in ambient air. We employed a unique setup, to simultaneously measure hygroscopic growth of different particle sizes at subsaturated conditions and CCN activation at supersaturated conditions on the same aerosol sample flow, in order to investigate the potential presence and direction of a discrepancy in κ-values between these humidity regimes. A similar approach has previously been used by Herich et al. (2009). Different relative L-OS 250 mixing ratios with ammonium sulphate (AS), an ubiquitous inorganic component in atmospheric aerosols were investigated with the setup. We also measured aqueous surface tension of bulk solutions of L-OS 250 and mixtures with AS, in particular to investigate the impact of a possible L-OS 250 surface activity on hygroscopic properties and cloud activation thermodynamics, as determined from equilibrium Köhler theory. Specifically, we aimed to establish whether the volume additive Zdanovskii–Stokes–Robinson (ZSR) mixing rule (Petters and Kreidenweis, 2007) is applicable for these particular particles, and whether there is any detectable change in the aerosol – water interaction properties with particle mixing state, in terms of humidity and particle composition and size.

ACPD
15, 17317–17365, 2015

2 Methods

2.1 Synthesis of limonene-derived organosulfates

L-OS 250 isomers were synthesized using the method described in more details by Cavdar and Saraçoğlu (2009) for synthesis of hydroxy sulfate esters by ring opening of epoxides with sodium hydrogen sulfate. Approximately 0.61 g limonene oxide was dissolved in 20 mL dried dichloromethane (CH_2Cl_2). Next, 1.10 g dried sodium bisulfate ($NaHSO_4$) was added to the reaction solution under magnetic stirring. The mixture was left at room temperature for 4–5 days for reaction, while the reaction environment was kept inert using nitrogen gas. The reaction scheme for the synthesis is given in Fig. 1.

Following synthesis, the product was purified by solid phase extraction on an ion exchange hydrophilic column (Strata-X-A 33u polymeric strong anion, Phenomenex) using a solvent sequence of 10 % acetonitrile in MilliQ water followed by acetonitrile and chloroform.

Based on analysis using an ultra-high performance liquid chromatograph coupled to a quadrupole time-of-flight mass spectrometer through an electrospray ionisation inlet (UHPLC-ESI-q-TOF-MS) running in either positive or negative ionization mode, it was estimated that an approximately 90 (±5) % pure sample of L-OS 250 isomers was obtained in the acetonitrile fraction, the 10 % impurities being by-products of organosulfates with MW 268 and MW 384 (chromatograms from the UHPLC-ESI-q-TOF-MS analysis are given in Supplement).

2.2 Measurement of surface tension

Aqueous solutions of L-OS 250 and mixtures of L-OS 250 and AS (Sigma-Aldrich ≥ 99 %), were prepared in MilliQ water (resistivity of 18.2 MΩcm at 25 °C) for measurement of surface tension, σ. For each solute composition, 9 or more solutions of different concentrations were made to obtain measurements over a broad concentration range (see details in Table 1).

ACPD
15, 17317–17365, 2015

Surface tension of each solution was measured with a FTÅ 125 pendant drop tensiometer, with an overall uncertainty of ±2 %. Measurements were done over a concentration range capturing the transition region of solution surface tension as it changes from the pure water value to the level of maximum obtainable surface tension reduction. Approximately 40 pictures were taken of each pendant drop and the surface tension was calculated based on the pictures by the programme FRÅ32. The surface tension reported here, resulted from analysis of three succeeding droplets, where the relative standard deviation of the surface tension did not exceed 1 %. Measured surface tension was parametrized as a function of ternary solution composition according to the equation previously used by Prisle et al. (2010b), here in the form:

$$\sigma = \sigma_w - a \times R \times T \times \mathrm{Ln}\left(1 + \frac{C_{\mathrm{L-OS250}}}{b}\right) \quad (1)$$

where σ_w is the surface tension of water, $C_{\mathrm{L-OS250}}$ is the molar concentration of L-OS 250, R is the universal gas constant in $\mathrm{J\,K^{-1}\,mol^{-1}}$, T is the temperature in Kelvin, Ln is the natural logarithm (to the base of e) and a and b are the Szyskowski equation fitting-parameters, which were fitted as dependent on solute mixing ratio, as:

$$a = a_1 + a_2 \times \frac{C_{\mathrm{AS}}}{C_{\mathrm{AS}} + C_{\mathrm{L-OS250}}} \quad (2)$$

$$b = b_1 + b_2 \times \frac{C_{\mathrm{AS}}}{C_{\mathrm{AS}} + C_{\mathrm{L-OS250}}} \quad (3)$$

where C_{AS} is the molar concentration of AS. The values for a_1, a_2 and b_1 and b_2 are given in Sect. 3.1.

2.3 Parallel H-TDMA/CCNC measurements

To study the hygroscopic properties and the CCN activation of particulate L-OS 250 and their mixtures with AS, a unique laboratory set-up was built, enabling parallel measure-

ACPD
15, 17317–17365, 2015

ments of both subsaturated water uptake and supersaturated cloud droplet activation for the same aerosol sample.

An atomizer (TOPAS ATM 220) was used to generate particles from aqueous solutions comprising L-OS 250 and AS in different relative mixing ratios. Each solution was prepared with de-ionized and purified water (18.2 MΩcm). The solute compositions (relative L-OS 250 and AS mass fractions) and total solute concentrations (C, [g(solute)/L(solution)]) are given in Table 2. Following atomization, the aqueous aerosol was dried by passing through a diffusion dryer containing silica gel, resulting in a dry aerosol with relative humidity (RH) in the range 4–7 %. It is assumed that particles at this RH are essentially water-free, and furthermore that their dry compositions reflect the relative solute mass fractions of the respective atomized solutions. At this point, the flow of dry particles was split two ways for parallel measurements of water uptake ability with a Hygroscopicity Tandem Difierential Mobility Analyzer (H-TDMA) and cloud droplet activation with a Cloud Condensation Nuclei counter (CCNC). A schematic of the water uptake characterization setup is shown in Fig. 2. Dry gas (N_2) was applied after atomization to dilute the particle concentration.

The hygroscopic growth factor (HGF) of the generated particles was studied with the fifth generation University of Helsinki Volatility Hygroscopicity Tandem Difierential Mobility Analyzer (VH-TDMA) (Hong et al., 2014), where the volatility mode was deactivated so the instrument functions solely in hygroscopicity mode. The dry particles were charged by a neutralizer and passed through a Difierential Mobility Analyzer (DMA1, Hauke type), where a monodisperse aerosol distribution was selected, based on the electrical mobility of the particles. For each particle composition, four individual dry sizes were selected: 30, 60, 100 and 145 nm. The flow of monodisperse particles was then split into two ways, one going into a humidifier while the other one bypassing the humidifier. The humidifier exposed the particles to an environment with four different set RHs of 80, 85, 90 and 93 %.

Number size distribution data from both routines were measured using two similar systems, each including a Differential Mobility Analyzer (DMA, Hauke type), scanning

ACPD
15, 17317–17365, 2015

the size distribution of the particles, and a condensation particle counter (CPC, TSI 3010 and TSI 3772), counting the number concentration of particles.

The HGF of the particles at each RH was obtained as the ratio of the size distribution of the humidified (D_{wet}) to dry (D_{dry}) particles (Cruz and Pandis, 2000):

$$\mathrm{HGF(RH)} = \frac{D_{wet}(\mathrm{RH})}{D_{dry}} \quad (4)$$

The H-TDMA was calibrated prior to the measurements using pure ammonium sulfate particles with sizes 30, 60, 100 and 145 nm at dry conditions. The obtained data in dry condition was used to calibrate the measured raw data at RHs in other regimes based on the algorithm introduced by Gysel et al. (2009). Furthermore, the measured growth factor distribution data was inverted using the piecewise linear inversion approach (Gysel et al., 2009) by the software Igor Pro to obtain the HGFs.

For each particle dry size, four to six measurements of the HGF were made at each RH and the relative standard deviation between these measurements was below 3 % for all compositions. This standard deviation accounts for uncertainties related to the experimental setup, including particle size selection and RH set point, as well as uncertainties connected with the data inversion process. Error bars presented in the following sections on reflect the variations between these measurements according to the observed relative standard deviations (±2 standard deviation). The standard deviation found here are in line with a previous study, estimating uncertainties on HGFs to be below 5 % (Massling et al., 2009).

The ability of the generated particles to activate into cloud droplets at supersaturated conditions was measured with a CCNC from Droplet Measurement Technologies (DMT, model CCN-100) attached with a Hauke-type DMA (DMA3). After passing through a neutralizer, the dried particles were transferred to DMA3 (see Fig. 1) from which a monodisperse particle distribution was obtained. The particle flow was then split into two lines, one going into a CPC (TSI, 3010), counting the total number concentration of particles, and one going to the CCNC, counting the number concentration

ACPD
15, 17317–17365, 2015

of particles that activate or become droplets larger than 1 µm at a given supersaturation (SS). CCN activation spectra were measured at thirteen different SSs, ranging from 0.099 to 0.922 % (corresponding to 100.099 to 100.922 % RH). The fraction of activated particles to total particles was thus obtained as a function of the particle dry size from the activation spectra. Activation spectra were corrected for multiply charged particles simultaneously selected in DMA3 and subsequently fitted using a sigmoidal function as done by Paramonov et al. (2013). From the fitted sigmoidal curve, the critical particle diameter (d50) was then determined. d50 for all SS was measured twice for all particle compositions except 90 % L-OS 250, for which SS was only measured once.

The nominel SS given by the CCNC was corrected to obtain the actual SS profile created in the instrument, based on measurements with AS following suggestions by Rose et al. (2008). Information regarding the calibration is given in Supplement. Regarding uncertainties on the measurements, it is estimated that the particle size-selection in the DMA has an uncertainty of 3 % and based on previous studies it is estimated that the uncertainty on the SS in the CCNC after calibration has a maximum value of 5 % of SS (Rose et al., 2008; Asa-Awuku et al., 2009). Error bars presented in the following sections on critical particle diameter reflect these uncertainties.

2.3.1 Calculation of κ

The critical diameters obtained from the CCN measurements and the HGFs obtained from the H-TDMA measurements were used to calculate an effective hygroscopicity parameter, κ, for all particle sizes, compositions, and humidity conditions. According to κ–Köhler theory, the κ parameter relates the dry diameter of particles of a specific chemical composition to the water uptake at a given RH or SS (Petters and Kreidenweis, 2007). Hence, κ for example also expresses the influence of chemical composition on CCN activity.

ACPD
15, 17317–17365, 2015

From the HGF (H-TDMA experiment), κ was calculated by the equation given below (Hong et al., 2014):

$$S(D_{\mathrm{wet}}) = \frac{\mathrm{HGF}^3 - 1}{\mathrm{HGF}^3 - (1-\kappa)} \exp\left(\frac{4\sigma \mathrm{MW_W}}{RT\rho_{\mathrm{W}} D_{\mathrm{dry}} \mathrm{HGF}}\right) \quad (5)$$

where $S(D_{\mathrm{wet}})$ is the saturation ratio, here it is the RH set in the H-TDMA measurements, HGF is the hygroscopic growth factor obtained from H-mode measurements, D_{dry} is the particle dry diameter, D_{wet} is the droplet diameter, σ is the droplet surface tension, ρ_{W} and $\mathrm{MW_W}$ are the density and molar mass of water, respectively, R is the universal gas constant, T is the inlet temperature.

For each dry size, RH and particle composition, HGF was measured four to six times, hence four to six κ-values were obtained. In the following sections κ for each composition at a given RH and dry size is represented as the mean κ-values from these measurements. The standard deviation on the mean κ-value was below 7 % for all compositions except for pure L-OS 250 where the standard deviation was up to 36 %. In the following sections error bars represent ± two standard deviations on the mean κ.

From the CCN measurements, κ was found using the equation (Petters and Kreidenweis, 2007; Rose et al., 2010).

$$S(D_{\mathrm{wet}}) = \frac{D_{\mathrm{wet}}^3 - D_{\mathrm{dry}}^3}{D_{\mathrm{wet}}^3 - D_{\mathrm{dry}}^3(1-\kappa)} \exp\left(\frac{4\sigma \mathrm{MW_W}}{RT\rho_{\mathrm{W}} D_{\mathrm{wet}}}\right). \quad (6)$$

Equation (6) was used to solve critical supersaturation for each particle dry size found in the experiments by changing κ and droplet diameter, D_{wet}, until the difference between calculated and calibrated supersaturation was at a minimum. Reported CCN κ-values are the κ-values resulting in minimum difference.

We calculate κ assuming the surface tension of pure water in Eqs. (5) and (6) above. Any effects of surface tension reduction in the droplets on water uptake and CCN activation are therefore captured in the variation of the corresponding effective κ-values

ACPD
15, 17317–17365, 2015

determined from our measurements. The uncertainty on the CCN-derived κ-values was estimated to 10 % (double the uncertainty on SS) and error bars on CCN-derived κ presented in the following sections represent this uncertainty.

Volume additive κ-values were calculated for particles of mixed composition, based on the Zdanovskii–Stokes–Robinson (ZSR) relation (Stokes and Robinson, 1966), by applying the κ-values for pure AS and L-OS 250 according to their estimated respective bulk volume fractions as previously done by for example Gysel et al. (2007), Petters and Kreidenweis (2007), Swietlicki et al. (2008) and Kristensen et al. (2014).

$$\kappa = \sum_i \varepsilon_i \kappa_i \tag{7}$$

Here, ε_i is the volume fraction of component i in the particle and κ_i is the intrinsic κ-value for component i in its pure form. The volume fraction is calculated from the mass fraction and the density of each component. The bulk mass density of AS is well known as 1.77 g cm^{-3} but to the best of our knowledge the density of L-OS 250 is currently unknown. Ambient organic aerosol mass densities are generally observed to be between 1.2 and 1.7 g cm^{-3} (Hallquist et al., 2009) and a density of 1.176 g cm^{-3} was found for sodium dodecyl sulphate, SDS (Prisle et al., 2011 and references herein), a surfactant with a sodium sulfate group (SO_4Na) considered to be similar to the sulfate group (HSO_4) in organosulfates. Hence, here we calculate additive κ-values assuming a density of 1.176 and 1.7 g cm^{-3} for L-OS 250 to cover this potential range. The volume additive κ-values were calculated for the specific purpose of investigating the validity of the additivity assumption for calculating κ-values for the L-OS 250/AS system.

2.4 Köhler modelling

Equilibrium growth by water uptake and cloud droplet activation of the studied particles from Köhler theory as described in Prisle et al. (2010b). Following κ was calculated from the modelled HGF and SSc using Eqs. (5) and (6) respectively.

ACPD
15, 17317–17365, 2015

Three different model approaches, previously introduced by Prisle et al. (2010b) were used to assess the effects of surface tension reduction and surfactant bulk-to-surface partitioning on the L-OS 250 water uptake. First, bulk-to-surface partitioning and surface tension effects are both ignored (σ_w), which in particular means that the droplet surface tension in Eq. (6) is taken as that of pure water. Second, reduction of droplet surface tension from L-OS 250 is considered, but the influence of bulk-to-surface partitioning is still ignored (σ_b). This means using the concentration dependent surface tension (Eq. 1) according to the total droplet concentration of L-OS 250. Third, bulk-to-surface partitioning is considered in the evaluation of the droplet bulk phase composition and surface tension (σ_p). This means that bulk solution concentrations (κ and droplet surface tension) change when the surfactant partitions to the droplet surface.

Droplet solution concentrations are calculated from the number of moles of each species (water, AS and L-OS 250), while assuming partial dissociation for ammonium sulphate ($\nu \sim 2.3$ based on the parametrisation presented by Prisle, 2006) and no dissociation for L-OS250 ($\nu = 1$). Both AS and L-OS 250 are assumed to be fully dissolved at all relevant droplet concentrations and droplet solutions are also assumed to be ideal, due to the current lack of explicit information on non-ideal solution interactions involving L-OS 250. Mass mean molecular weight of 255.3 Da was assumed for L-OS 250, based on the 10 % impurities. Droplet surface tension is calculated using Eq. (1) when surface tension effects are accounted for, using the L-OS 250 bulk concentration evaluated either with or without consideration of bulk-to-surface partitioning; otherwise the constant surface tension value of pure water is used. Since the fit (Eq. 1) can give negative surface tension values at high L-OS 250 concentrations, the minimum surface tension have been limited to 0.020 N m^{-1}. When bulk-to-surface partitioning is accounted for, droplet bulk solution concentrations are solved from the Gibbs adsorption equation as described in detail by Prisle et al. (2010b). This requires that the surface tension gradient is well-defined and non-zero, which in this case specifically means that surfactant bulk-to-surface partitioning cannot be evaluated for solution compositions resulting in droplet surface tensions below 0.020 N m^{-1}. This corresponds to the physical

ACPD
15, 17317–17365, 2015

situation of constant surface tensions obtained for solutions above the so-called critical micelle concentration, where the aqueous surface is saturated in adsorbed surfactant and no further bulk-to-surface partitioning takes place (for more details, see Prisle et al., 2010b).

3 Results and discussion

3.1 Surface tension

Figure 3 shows the surface tension of aqueous solutions of L-OS 250 and five mixtures of L-OS 250 and AS, as a function of the L-OS 250 molar concentration. L-OS 250 decreased the surface tension of aqueous solution from that of pure MilliQ water ($73\,mN\,m^{-1}$ at 20 °C) considerably. Even at a concentration of $0.0025\,mol\,L^{-1}$ the surface tension was decreased to $55.5\,mN\,m^{-1}$. The surface tension further decreased to $39.4\,mN\,m^{-1}$ when the L-OS 250 concentration increased to $0.24\,mol\,L^{-1}$. Surface tension of the mixed L-OS 250 and AS solutions with $\leq 50\,\%\,w/w$ AS converges toward the surface tension of pure aqueous L-OS 250, while the surface tension for the mixed solutions with $\geq 80\,\%$ AS was lower than for the solutions of pure L-OS 250 with the same aqueous concentration. Previous studies have shown that addition of AS to pure water increased the surface tension (Lee and Hildemann, 2013; Matubayasi, 2013), however a decrease in surface tension of an organic solution when AS is added has been observed. For example, Ekström et al. (2009) found the surface tension of solutions of mannitol and methylerythritol to decrease with addition of $17\,\%\,w/w$ AS, whereas the surface tension of solutions of adipic acid and methylthreitol increased with the same mass addition of AS. The difference between their observations and the present can be qualitatively explained by differences in surface activity, impact on aqueous surface tension and effects interactions with the inorganics of the different organics involved. The additional surface tension reduction observed at high AS concentration in the present study is consistent with a salting out effect, where the presence of AS

ACPD
15, 17317–17365, 2015

in solution decreases the solubility of L-OS 250, hereby forcing L-OS 250 towards the solution surface.

For the investigated system, the lowest surface tension was observed for the L-OS 250 solutions with 90 % AS at all L-OS 250 concentrations, where the surface tension dropped from approximately 73 to 33 mN m^{-1} over the concentration range of 0.0001 to 0.05 mol L^{-1} L-OS 250. Interestingly, the surface tensions of the L-OS 250 solutions with 95 % w/w AS were increased compared to the 90 % w/w AS of the same L-OS 250 concentration, over the full concentration range probed and converged towards the surface tension of pure L-OS 250 at concentrations lower than 0.005 mol L^{-1}. These observations suggest the presence of non-additive effects of L-OS 250 and AS affecting solution surface tension, since the surface tension at a given L-OS 250 concentration does not decrease monotonically with AS concentration over the full range of L-OS 250/AS mixing ratios from 1–0. At 90 % AS, salting out of the organic by AS appears to be the dominant effect causing surface tension to decrease below the additive effects of each solute components separately in solution, whereas at 95 % AS the increase in surface tension caused by AS is no longer fully counteracted by surfactant salting out.

Measured surface tensions were parametrized as a function of ternary solution composition according to Eq. (1). The fits are plotted in Fig. 3 together with measured data and the fitting parameters are $a_1 = 1.86 \times 10^{-6}$ mol m^{-2}, $a_2 = 5.78 \times 10^{-7}$ mol m^{-2}, $b_1 = 1.30 \times 10^{-4}$ mol L^{-1}, $b_2 = 1.67 \times 10^{-6}$ mol L^{-1}. The difficulty to capture the composition-dependent surface tension variation over the full range of concentrations again indicates that the combined influences of L-OS 250 and AS on ternary aqueous surface tension are not linearly additive, as is also clear from the trend in the measurements. This might be expected for two components of very different molecular structures and behaviour in respective binary aqueous solutions.

ACPD
15, 17317–17365, 2015

3.2 Hygroscopic growth factor

Figure 4 shows HGF of laboratory generated particles of L-OS 250, AS and their mixtures as a function of RH. The HGF is shown for particles of four dry sizes (30, 60, 100 and 145 nm) being exposed to 80–93 % RH.

All six particle compositions showed hygroscopic growth at the selected RHs, and the HGF increased with increasing RH in each case, as expected for particles with non-vanishing hygroscopicity.

Only weak hygroscopic growth was observed for the pure L-OS 250 particles with HGF increasing from approximately 1.0 (no growth) at 80 % RH to 1.2 at 93 % RH. There are no indications of deliquescence, as water uptake occurs smoothly over the given RH range. To the best of our knowledge the aqueous solubility of L-OS 250 is currently not characterized. Our present data are consistent with a modest L-OS 250 solubility, leading to a saturated solution with a water activity of about 0.85 at the onset of hygroscopic growth. The HGF of pure AS particles on the other hand increased from approximately 1.4 to 1.9 over the same RH range, consistent with the high water solubility and well-documented hygroscopic properties and deliquescence RH (DRH) of AS of 79.9 (±0.5) % at 295 K (Seinfeld and Pandis, 2006).

For the mixed particles, the HGF corresponding to a given dry particle size and RH increased with increasing weight percentage of AS, in accordance with an increasing contribution of the more hygroscopic component. For mixtures with $\geq 20\,\% w/w$ AS, the overall HGF converged towards the HGF of pure AS for all particle sizes. It must be kept in mind, that when a particle with presumably $80\,\% w/w$ of L-OS 250 or some other organic demonstrates the same HGF as a pure AS particle, it does not imply that the organic has no intrinsic hygroscopicity in the mixture, but rather, that the resulting impact of the organic in the mixed particle is similar to the hygroscopic properties that would arise from the same particle fraction being composed purely of AS. In accordance with Köhler theory, any reduction of droplet surface tension from L-OS 250 should increase particle hygrocopicity. This therefore means that surface tension effect

ACPD
15, 17317–17365, 2015

of L-OS 250 in our experiments appear to compensate for a possible decrease in direct impact on water activity from the larger molecular size, lower solubility and lower dissociation degree of L-OS 250, compared to AS.

In general, the dry size of the particles were observed to have little or modest influence on the measured HGF, however, for the particles of pure L-OS 250 and L-OS 250 with 10 % w/w AS, the largest HGF was observed for the smallest particle sizes compared with the larger particles. For the pure AS particles and particles with ≥ 20 % w/w AS, the opposite behaviour was seen, where the largest HGFs were measured for the largest particles. This further supports our inferences related to effects of organic solubility vs. surface activity: for particles with the highest fractions of L-OS 250, there could be kinetic effects of dissolution present, increasing the amount of dissolved material in the smallest particles, compared to the larger ones. Conversely, for particles with larger amounts of AS relative to L-OS 250, the hygroscopicity of the inorganic likely negates any effects of limited organic solubility. The size dependency for these particles may be related to effects of organic depletion from bulk-to-surface partitioning decreasing the relative amount of hygroscopic material in the droplet bulk of the smallest particles, compared to the larger ones (Prisle et al., 2010b).

Hämeri et al. (2002) have previously observed a similar effect of mixed organic and inorganic particles showing an overall particle hygroscopicity close to that of pure AS, in that the HGF measured for particles of malonic acid with 50 % w/w AS and succinic acid with 50 % w/w AS coincided with HGF for pure AS. The acids studied by Hämeri et al. (2002) are however hygroscopic and only weakly surface active, hence this behaviour is likely due to the coincidence of the effects of different mechanisms than in this work, in particular the relative effects of the organic and inorganic on droplet water activity. In our experiments the HGFs already coincide with the ones for pure AS at as low as 20 % w/w AS, pointing to the significance of surface tension reduction effects for increasing the organic contribution to particle hygroscopicity, since L-OS 250 is a much stronger surfactant than the acids studied by Hämeri et al. (2002).

ACPD
15, 17317–17365, 2015

3.3 Critical particle diameter

Figure 5 shows the measured critical supersaturation (SSc) as function of dry particle diameter (D_{dry}) for the six different dry particle compositions studied. Particles of all compositions could activate into cloud droplets in the investigated SS range and the SSc for activation decreased with increasing dry particle diameter as expected from equilibrium Köhler theory. Pure L-OS 250 particles activated at larger dry diameters compared to particles of pure AS at all selected SS, for example at a SS of 0.16 % pure L-OS 250 activated at a dry diameter of 170 nm whereas AS activated at a dry diameter of 93 nm. The curves for all six compositions follow the Köhler slope of approximately −3/2 in log-log space. According to equilibrium Köhler theory, this means that no explicit size-dependent effects are present in the obtained CCN spectra (Seinfeld and Pandis, 2006). Pure AS and L-OS 250 with 80, 50 and 20 % *w*/*w* AS had a slope of −3/2, whereas the slope for pure L-OS 250 and L-OS 250 with 10 % *w*/*w* AS were slightly smaller (approximately −1.4), consistent with the presence of a modest size-dependent effect attributed to L-OS 250.

As was also observed for the measured subsaturated HGF, supersaturated activation properties of the mixed particles were dominated by AS, where the activation dry diameter at all SSs decreased with increasing weight percentage of AS. For particles with ≥ 20 % *w*/*w* AS the activation dry diameter is essentially the same as for pure AS.

Previous studies of mixed organic and inorganic particles showed similar observations of a decrease in activation dry diameter with increasing amount of inorganics. For example, Prisle et al. (2010b) found the activation diameters of mixed surfactant (e.g. sodium octanoate, sodium decanoate, sodium dodecanoate and sodium dodecyl sulfate) and sodium chloride (NaCl) particles to decrease with increasing NaCl mass fraction in the particles, when investigating surfactant/NaCl systems with 5 to 80 % *w*/*w* NaCl. However in contrast to the present study, the activation diameters did not coincide for any of the different surfactant/NaCl compositions investigated, indicating that the full cancellation of different opposing effects did not occur in their study.

ACPD
15, 17317–17365, 2015

3.4 κ-values

κ-values were calculated based on the H-TDMA measurements using Eq. (5) and based on the CCN measurements using Eq. (6) as well as using the ZSR-based additive formula (Eq. 7). Furthermore, H-TDMA and CCN experiments were modelled from equilibrium Köhler theory employing three different sets of assumptions, as explained in Sect. 2.4 above and the corresponding κ-values were calculated from the modelled HGF and SSc using Eqs. (5) and (6) respectively.

3.4.1 H-TDMA derived κ

Figure 6 shows $\kappa_{\text{H-TDMA}}$ as function of RH and dry particle size (D_{dry}) for the six compositions of L-OS 250 with AS investigated. The obtained κ-values for particles of all six chemical compositions at the four RHs showed a consistent size dependence, where κ decreased with increasing particle size. The error bars, here representing ± two standard deviations, on individual κ-values for a given composition show some overlap for the high AS fraction composition, whereas no overlap is observed for pure L-OS 250 and L-OS 250 with 10 % w/w AS, suggesting that this trend may be statistically significant for at least the latter two. To our knowledge, this is the first time that a decrease in $\kappa_{\text{H-TDMA}}$ with increasing dry particle size has been reported for particles of the same chemical composition.

Some studies of ambient aerosols have on the contrary showed that κ-values increase with particle size. For example, Holmgren et al. (2014) and Wu et al. (2013) found $\kappa_{\text{H-TDMA}}$ to increase with particle size during field campaigns in France and Germany, respectively. However, for field measurements, the chemical composition of the particles with all likelihood changes with size and with time, hence the change in κ observed with increasing particle size in the field studies is probably a result of changing chemical composition. In this study, particles of different size were formed from atomization of the same solution, hence, ideally they should have the same chemical composition. If this is the case, then the observed trend implies that the smaller par-

ACPD
15, 17317–17365, 2015

ticles are more hygroscopic than larger ones of the same chemical composition. This dependence may in turn be a true size dependence, resulting from a change in surface effects or dissolution kinetics with particle size. It should be mentioned, that the observed size dependence could potentially be an indirect effect of a changing chemical composition or from an artefact in our experiments. From the HGF measurements a bimodal size distribution was observed for the mixed L-OS 250/AS particles, indicating that the particles may be externally mixed, thus it is possible that droplets formed with the atomizer from mixed L-OS 250/AS solutions have different chemical composition due to the surface activity of L-OS 250. The same could in principle be true for the pure L-OS 250 particles, since approximately 10 % impurities (of two other organosulfates) were present here, however, these impurities are very similar in structure to L-OS 250. On the other hand it cannot explain the observed size dependence of the pure AS particles which should be fully soluble and not surface active in any case. We therefore do not believe that changing particle composition is the main cause of the observed particle size dependency in measured κ-values. Based on our results alone and the relatively modest size dependence observed, we cannot give the conclusive statement that smaller particles are more hygroscopic than larger ones of the same chemical composition. However the results present the possibility and further studies should be conducted.

Regarding RH, $\kappa_{\text{H-TDMA}}$ for pure L-OS 250 increased significantly ($\Delta\kappa/\kappa_{\text{RH93\,\%}} \times 100\,\% = 44$, 72, 92 and 95 % for 30, 60, 100 and 145 nm particles respectively), when RH increased from 80 to 93 % humidity. This increase in $\kappa_{\text{H-TDMA}}$ could be caused by increased dissolution of L-OS 250. At low RH (here 80 %), the water content in the droplets may not be high enough to dissolve the L-OS 250 particle entirely, resulting in a mixed liquid- and solid-phase droplet. Both Henning et al. (2012) and Zardini et al. (2008) have previously suggested that phase separation could make aerosol hygroscopicity RH dependent and Henning et al. (2012) found that soot particles coated with solid succinic acid resulted in no hygroscopic growth whereas soot particles coated with liquid/dissolved succinic acid resulted in hygroscopic growth, suggesting that the

ACPD
15, 17317–17365, 2015

increase in $\kappa_{\text{H-TDMA}}$ observed here could also be caused by gradual dissolution of L-OS 250 with increasing RH. This effect will be discussed further in Sect. 3.4.3.

For the pure AS particles and the L-OS 250 particles with 10, 50 and 80 % w/w AS, increasing subsaturated RH showed no clear effect on $\kappa_{\text{H-TDMA}}$. For these compositions, the $\kappa_{\text{H-TDMA}}$ appeared to be within in a stable range, independent of RH. For L-OS 250 particles with 20 % w/w AS, $\kappa_{\text{H-TDMA}}$ decreased with increasing RH. This changing behaviour of κ with respect to RH for the different particle compositions may be due to a change in interactions between AS and L-OS 250 with changing mass fraction, which could influence the particle water activity.

$\kappa_{\text{H-TDMA}}$ showed a clear increase with increasing mass fraction of AS, where $\kappa_{\text{H-TDMA}}$ for mixtures with $\geq$ 20 % AS converged towards the values of pure AS. As discussed by Sjögren et al. (2008), interaction of inorganic and organic species can increase the overall particle hygroscopicity and thus the apparent hygroscopicity of organic compounds, hence the high κ-values observed for the mixed particles with $\geq$ 20 % w/w AS, that cannot be explained by increasing AS fraction alone is expected to be a result of such interactions. The $\kappa_{\text{H-TDMA}}$ for pure L-OS 250 (0.002 to 0.09) correspond to weakly hygroscopic organic compounds according to Petters and Kreidenweis (2007). L-OS 250 contains an alcohol group and a sulfate group, which are both polar; however the molecule contains a hydrophobic ring structure, hence it is not surprising that the hygroscopicity of L-OS 250 is modest. The $\kappa_{\text{H-TDMA}}$ for pure AS was here measured to be between 0.42 and 0.58, in line with previous studies, where κ for AS is in the range 0.33 to 0.72 (Clegg et al., 1998; Koehler et al., 2006; Carrico et al., 2008).

3.4.2 CCN-derived κ

Figure 7 shows the CCN-derived κ-values as a function of SSc for the different particle compositions. In general, κ_{CCN} increased with increasing mass fraction of AS in the particles, and those with $\geq$ 20 % w/w AS have κ-values converging towards those of pure AS, exactly as was also found for $\kappa_{\text{H-TDMA}}$. This trend is therefore consistent over the whole humidity range investigated. κ_{CCN} for the pure L-OS 250 particles showed

ACPD
15, 17317–17365, 2015

a weak increase with SS, implying a corresponding decrease of κ with increasing particle size, as the larger particles of a given composition activate at lower supersaturation conditions. κ_{CCN} increased from 0.095 to 0.145 when the SSs increased from 0.168 to 0.922 %, corresponding to particle diameters 170 and 47 nm, respectively (see Fig. 7). κ_{CCN} for the L-OS 250 particles with 10 % w/w AS also show a weak increase with SS, rising from 0.18 to 0.23 over the selected SS range. However, including the uncertainty on $\kappa_{CCN,}$ the increasing trend for L-OS 250 and L-OS 250 with 10 % w/w AS is likely not significant. For the pure AS particles and the particles with $\geq$ 20 % w/w AS, κ_{CCN} showed no clear sign of increasing or decreasing trend with SS, but fluctuated within a range for each particle composition (0.49 to 0.57 for L-OS 250 with 20 % w/w AS, 0.50 to 0.59 for L-OS 250 with 50 % w/w AS, 0.50 to 0.60 for L-OS 250 with 80 % w/w AS and 0.51 to 0.59 for pure AS), where the individual κ_{CCN} fell within the uncertainty range of each other. Since the size dependency is strongest for pure L-OS 250, this suggests relation to properties of the organic, such as surface activity effects. We argue that a mean κ_{CCN} for each particle composition can be used to represent κ_{CCN} over the entire SS range of 0.099–0.922 % investigated, as the individual κ_{CCN} fall within the overall uncertainty, and since the Köhler slopes obtained from the SSc curves are approximately $-3/2$ for all particle compositions, indicating the absence of significant size-dependent effects on SSc. Hence, in the following, κ_{CCN} for each composition is given as the mean κ_{CCN} ($\pm$1 standard deviation) over the investigated SS range. In Table 3, the mean, minimum and maximum κ_{CCN} as well as standard deviation of κ_{CCN} is given.

3.4.3 Comparison of H-TDMA and CCN derived κ

Comparing $\kappa_{H\text{-}TDMA}$ and κ_{CCN} of each of the six particle compositions (see Fig. 8), it is clear that κ-values for pure L-OS 250 are higher for supersaturated (CCN) than for subsaturated (H-TDMA) conditions. This is observed for all RH and particle dry sizes measured with the H-TDMA. We note that the difference in κ between the two methods became smaller with increasing RH, meaning that at higher RH, $\kappa_{H\text{-}TDMA}$ for

ACPD
15, 17317–17365, 2015

L-OS 250 approach κ_{CCN}, as expected if there is indeed a dissolution effect present. As mentioned in Sect. 3.4.1, the increase in $\kappa_{H\text{-}TDMA}$ for L-OS 250 with increasing RH could be caused by increased dissolution of L-OS 250, which would be consistent with the indications of its modest water solubility discussed above. This explanation is supported by the observation of $\kappa_{H\text{-}TDMA}$ approaching κ_{CCN} with increasing RH. It is therefore suggested that the low $\kappa_{H\text{-}TDMA}$ for L-OS at 80, 85 and 90 % RH is caused by incomplete dissolution of L-OS 250 resulting in a mixed solid-/aqueous-phase system.

The $\kappa_{H\text{-}TDMA}$ for L-OS 250 with 10 % AS coincide with κ_{CCN} for 30 and 60 nm particles whereas 100 and 145 nm particles have κ-values below the corresponding κ_{CCN}. For L-OS 250 particles with $\geq$ 20 % w/w AS, it was generally observed that $\kappa_{H\text{-}TDMA}$ for 30 nm particles were a bit higher than κ_{CCN}, whereas $\kappa_{H\text{-}TDMA}$ for 145 nm particles were lower than κ_{CCN} and finally $\kappa_{H\text{-}TDMA}$ for 60 and 100 nm particles were essentially the same as the obtained κ_{CCN}. An exception is found for pure AS at 90 % RH, and L-OS 250 with 20 to 80 % w/w AS at 93 % RH, where $\kappa_{H\text{-}TDMA}$ were below κ_{CCN} for the three larger particle sizes.

The trend of $\kappa_{H\text{-}TDMA}$ being smaller than κ_{CCN} has previously been observed in other laboratory studies investigating secondary organic aerosol hygroscopicity (Prenni et al., 2007; Petters et al., 2009; Massoli et al., 2010; Wex et al., 2010; Pajunoja et al., 2015), as well as in field measurements of ambient aerosol (Cerully et al., 2011; Hersey et al., 2013; Hong et al., 2014). The discrepancies between $\kappa_{H\text{-}TDMA}$ and κ_{CCN} found in the field studies were discussed by Hong et al. (2014), outlining different effects that could influence κ, first, the different degrees of dissolution of organics at sub- and supersaturated conditions, as well as potential phase separation of the particle and secondly the difference in instrumental design of the H-TDMA and CCNC, such as the residence time in the instrument relative to the aerosol equilibration time at the sub- and supersaturated conditions.

The difference between $\kappa_{H\text{-}TDMA}$ and κ_{CCN} can be explained from the first-mentioned dissolution effect, since the discrepancy is mainly observed for the pure L-OS 250 particles, whereas the L-OS 250 particles with $\geq$ 20 % w/w AS in general had the same

ACPD
15, 17317–17365, 2015

κ-values measured in the two saturation regimes, hence the interactions between AS and L-OS 250 are similar at sub- and supersaturation conditions at $\geq 20\,\%\,w/w$ AS. Close agreement between $\kappa_{\text{H-TDMA}}$ and κ_{CCN} have previously been found for ambient aerosols with high mass fraction of ammonium and sulfate ions (e.g. Good et al., 2010). This could imply that a given amount of organics in aerosols may influence the aerosol hygroscopicity to a different extend at sub- and supersaturated conditions and that application of a single κ value for a specific aerosol chemical composition many not be sufficient for describing particle hygroscopicity over the entire sub- and supersaturated humidity range.

3.4.4 Modelled κ

HGF and SSc values for L-OS 250, AS and four mixtures hereof investigated in our experiments were modelled from equilibrium Köhler theory employing 3 different sets of assumptions as described in Sect. 2.4 above:

1. Bulk-to-surface partitioning and surface tension effects are both ignored (σ_{w}).
2. Reduction of surface tension from the organic is considered, but effects of bulk-to-surface partitioning on droplet concentration are ignored (σ_{b}).
3. Bulk-to-surface partitioning is considered in the evaluation of the droplet bulk phase composition, and the impact on surface tension according to the resulting bulk concentrations is included (σ_{p}).

κ-values were then calculated from the modelled HGF- and SSc-values using Eqs. (5) and (6), respectively. The purpose was to examine if surface tension or surfactant partitioning can explain the observed hygroscopic behaviour for the investigated L-OS 250 containing particles. Furthermore, κ-values for the four L-OS 250/AS mixtures corresponding to κ at sub- and supersaturated conditions were modelled using the volume additive ZSR mixing rule (Eq. 7), using the measured mean κ-values of pure

ACPD
15, 17317–17365, 2015

L-OS 250 and pure AS and the respective volume fractions of the two compounds. To obtain particle volume fractions from experimental mass fractions, we ideally need the mixed particle density, estimated as the volume additive bulk mass density of different particle components. The density of L-OS 250 ($\rho_{L-OS250}$) is to the best of our knowledge unknown; hence the calculation was done using two different density cases for L-OS 250, 1.176 and 1.7 g cm^{-3}, as explained in Sect. 2.3.1. κ was modelled this way for both sub- and supersaturated conditions (see Fig. 9).

The left panel of Fig. 9 shows the additivity representation of κ (κ_{ZSR}) together with the measured values of $\kappa_{H\text{-}TDMA}$ and κ_{CCN}. κ_{ZSR} calculated using $\rho_{L-OS250}$ = 1.176 g cm^{-3} (κ_{ZSR_1}) resulted in κ-values closer to the measured values than did κ_{ZSR} calculated using $\rho_{L-OS250}$ = 1.7 g cm^{-3} (κ_{ZSR_2}) for all L-OS 250/AS compositions. κ_{ZSR_1} for L-OS 250 with 10 and 80 % w/w AS were reasonably close (±10 %) to $\kappa_{H\text{-}TDMA}$ for 145 nm particles and κ_{CCN}; however, for L-OS 250 with 20 and 50 % w/w AS, $\kappa_{H\text{-}TDMA}$ and κ_{CCN} fall in the range of 0.4–0.6, whereas κ_{ZSR_1} have values of 0.17 and 0.32 for H-TDMA and 0.23 and 0.37 for CCN respectively. For these compositions, the additivity formula thus yields a very poor representation of the variations in measured κ-values, suggesting that the additivity formula should only be used for compositions very close to pure L-OS 250 or pure AS.

κ-values, modelled using the σ_w, σ_b and σ_p representations, are similar in the subsaturated range and the values are practically independent of dry size and supersaturation. This behaviour is seen, because surface tension changes have negligible effect on the equilibrium relative humidity and surfactant bulk-to-surface partitioning is limited due to the low surface area to volume ratio for droplets conditioned at subsaturated humidities. As a result, the Köhler representation κ-values are similar to the ZSR κ-values and equally poor in representing the observed non-linear weight fraction dependency. This suggests that the non-linear composition dependency is caused by dissolution and non-ideal droplet interaction effects of L-OS 250, which are not accounted for in the Köhler models, rather than being a consequence of L-OS 205 surface activity.

ACPD
15, 17317–17365, 2015

One striking feature is that the bulk surfactant representation σ_b is clearly not able to predict measured aerosol water uptake and droplet activation in the supersaturated humidity range. This has been found consistently in previous studies of both pure surfactant and mixed surfactant/salt systems (Prisle et al., 2008, 2010b, 2011). Based on equilibrium Köhler theory, water uptake is increased, when droplet solution surface tension is decreased according to the bulk solution surface tension parametrisation, which leads to unrealistically large modelled κ-values for particles comprising L-OS 250. The σ_w representation is much better at reproducing experimental data, but again the model is not able to predict the non-linear composition dependency, since also this model is purely a bulk solution representation. Finally, the σ_p model is able to predict the magnitude of the pure L-OS 250 κ_{CCN}-value and also the increasing trend with increasing SS, but again the model is not able to predict the non-linear composition dependency. This strongly suggests that partitioning effects do in fact influence activation thermodynamics of L-OS 250, even if the overall κ-values may be subject to cancellation effects, as was found for other atmospheric surfactants (Prisle et al., 2008, 2010b), but is not a driver of variation in the water uptake in the sub- or supersaturated regimes.

These findings are in good agreement with those from Prisle et al. (2010b), who showed that bulk solution surface tensions should not be used for microscopic droplets without accounting for bulk-to-surface partitioning.

4 Cloud-forming effects of organosulfates

We have here outlined the hygroscopic properties and aqueous surface activity of L-OS 250. From our measurements, it was clear that L-OS 250 is indeed surface active and decreases the surface tension of water considerably, even for mixtures where the L-OS 250 concentration were as low as 5 % of total solute concentration. However, the low intrinsic κ-values for L-OS 250 showed the organosulfate to be modestly hygroscopic, hence in terms of water uptake, the significant surface activity must be countered by other effects in the droplets, such as limited water solubility. Based on the results pre-

ACPD
15, 17317–17365, 2015

sented here, the intrinsic cloud forming properties of pure L-OS 250 thus appear to be limited. On its own, L-OS 250 particles require significantly higher SS to activate into cloud droplets compared to the inorganic salts such as AS. On the other hand, L-OS 250 does not appear to inhibit the CCN activity of very active inorganics such as AS beyond displacing the AS mass in the aerosol, since he hygroscopic properties of mixtures of L-OS 250 and AS, converged towards the properties of pure AS, when AS composed $\geq 20\,\%$ w/w of the mixture. In fact, when particles with as much as 80 % by mass of L-OS 250 display the same water uptake properties as pure AS particles of the same size, it shows a significant contribution of the organic and/or its interactions with the inorganic. L-OS 250 is but one of many organosulfates found in the atmosphere, but we believe that the hygroscopic properties found for L-OS 250 in this study is a good representation for (at least some of the) other monoterpene-derived organosulfates, for example OS 250 derived from α-/β-pinene, L-OS 252 and L-OS 268, since they have structural similarities and few functional groups (see Fig. 10). Many organosulfates of atmospheric relevance contain additional hydroxyl groups or carboxylic acid groups and are composed of fewer carbon atoms than L-OS 250, for example OS 200 and OS 216 derived from isoprene (see Fig. 10). These organosulfates with additional hydroxyl/carboxylic acid groups are likely to be more hygroscopic, and therefore more prone to activate into cloud droplets, according to the recent study by Suda et al. (2014), showing that hygroscopicity of organics increases with addition of hydroxyl groups, carboxylic acid groups and hydroperoxide groups, in the given order. There is thus a need for further hygroscopicity measurements to investigate the atmospheric impact and cloud forming potential of smaller and more polar organosulfates, e.g those derived from isoprene.

5 Conclusions

We have here presented the first measurements of hygroscopic properties, CCN activity and aqueous surface tension properties for an atmospheric organosulfate. These

ACPD
15, 17317–17365, 2015

water interaction properties of L-OS 250, AS and mixtures hereof were examined in the laboratory at sub- and supersaturated conditions, using an instrumental setup that allows parallel measurements of HGF (with an H-TDMA) and of CCN activation (with a CCNC). HGF for L-OS 250 was found to increase from 1.0 (no growth) to 1.2 over the measured subsaturated humidity range from 80 to 93 %, showing that L-OS 250 can take up water in the subsaturated range. However compared to AS (HGF = 1.4 at 80 % RH and 1.9 at 93 % RH), the investigated L-OS 250 particles only showed weak hygroscopic growth. Measurement with the CCNC showed the ability of L-OS 250 to activate into cloud droplets; the critical diameters for L-OS 250 particles were 55–83 % larger than for pure AS, which is comparable to critical diameters for other atmospheric organics, that have previously been characterized. At both sub- and supersaturated conditions, the water uptake properties of mixed particles with $\geq 20\,\% \, w/w$ AS became similar to those of pure AS, showing that the contribution of L-OS 250 to the overall hygroscopicity of these mixed particles is not insignificant. The hygroscopicity parameter, κ, was calculated for the L-OS 250/AS system from both H-TDMA measurements and the CCN measurements, respectively, and $\kappa_{\mathrm{L-OS250}}$ was in the range 0.002–0.14, corresponding to weakly hygroscopic organics, whereas κ_{AS} was in the range 0.42–0.59, as expected for a hygroscopic salt. $\kappa_{\mathrm{H\text{-}TDMA}}$ was found to vary with particle size for all particle compositions, increasing with decreasing particle dry diameter. However, whether $\kappa_{\mathrm{H\text{-}TDMA}}$ is truly size dependent, or the size dependency is a result of an experimental artefact, cannot be concluded from these experiments alone. κ_{CCN} was larger than $\kappa_{\mathrm{H\text{-}TDMA}}$-values obtained from all RH and particle dry sizes for L-OS 250, which we explain by differences in the degree of dissolution of L-OS 250 in the particles at sub- and supersaturated conditions. For AS and mixed L-OS 250/AS particles κ_{CCN} and $\kappa_{\mathrm{H\text{-}TDMA}}$ were in the same range.

Surface tension measurements showed L-OS 250 to be surface active with the capacity to decrease the surface tension considerably in bulk aqueous solution. At an L-OS 250 concentration of 0.0025 mol L^{-1}, the surface tension of water was decreased by 24 % from the pure water value. The surface tension of L-OS 250 solutions with

ACPD
15, 17317–17365, 2015

a given organic concentration decreased with addition of AS, suggesting a salting out effect in bulk solutions.

Modelled κ, calculated from the volume additive ZSR mixing rule and from model predicted HGF and critical supersaturations, were not able to capture the observed non-linear composition dependency upon mixing with AS in the particle phase. The models accounted for different surface tension effects, so these are not the main reasons for the observations. This indicates that L-OS 250 solubility and droplet solution are non-ideal, which were not accounted for by the models, could be important for mixtures of the L-OS 250/AS system.

The study evaluates the cloud forming properties of atmospheric organosulfates derived from monoterpenes, but in order to cover the hygroscopic properties of the full range of atmospheric organosulfates more experiments are needed, especially with the smaller and more polar ones derived from isoprene.

The Supplement related to this article is available online at doi:10.5194/acpd-15-17317-2015-supplement.

Acknowledgements. This research was financially supported by NordForsk (Nordic Council of Ministers) through the Nordic Centre of Excellence Cryosphere–Atmosphere Interactions in a Changing Arctic Climate (CRAICC) and the VILLUM Foundation. The research leading to these results has received funding from the European Union Seventh Framework Programme (FP7/2007–2013) under grant agreement n°262 254 and via H2020 under ACTRIS2. The work was partly supported by the Office of Science (BER), U.S. Department of Energy via Biogenic Aerosols – Effects on Clouds and Climate (BAECC). N. L. Prisle gratefully acknowledges the personal funding received for this work from the Finnish Academy of Sciences (grant 257 411). The authors would also like to thank Ulla Wideqvist, Johan Ström and Hans Christen Hansson for use of the tensiometer at ITM, Stockholm University and Mikhail Paramonov for providing Matlab scripts for calculation of κ_{CCN} and help regarding calibration of the CCNC instrument.

ACPD
15, 17317–17365, 2015

References

Asa-Awuku, A., Engelhart, G. J., Lee, B. H., Pandis, S. N., and Nenes, A.: Relating CCN activity, volatility, and droplet growth kinetics of β-caryophyllene secondary organic aerosol, Atmos. Chem. Phys., 9, 795–812, doi:10.5194/acp-9-795-2009, 2009.

Carrico, C. M., Petters, M. D., Kreidenweis, S. M., Collett, J. L., Engling, G., and Malm, W. C.: Aerosol hygroscopicity and cloud droplet activation of extracts of filters from biomass burning experiments, J. Geophys. Res.-Atmos., 113, D08206, doi:10.1029/2007jd009274, 2008.

Cavdar, H. and Saraçoğlu, N.: Ring opening of epoxides with $NaHSO_4$: isolation of beta-hydroxy sulfate esters and an effective synthesis for trans-diols, Tetrahedron, 65, 985–989, doi:10.1016/j.tet.2008.11.092, 2009.

Cerully, K. M., Raatikainen, T., Lance, S., Tkacik, D., Tiitta, P., Petäjä, T., Ehn, M., Kulmala, M., Worsnop, D. R., Laaksonen, A., Smith, J. N., and Nenes, A.: Aerosol hygroscopicity and CCN activation kinetics in a boreal forest environment during the 2007 EUCAARI campaign, Atmos. Chem. Phys., 11, 12369–12386, doi:10.5194/acp-11-12369-2011, 2011.

Cheng, Y., Li, S. M., Leithead, A., Brickell, P. C., and Leaitch, W. R.: Characterizations of cis-pinonic acid and n-fatty acids on fine aerosols in the Lower Fraser Valley during Pacific 2001 Air Quality Study, Atmos. Environ., 38, 5789–5800, doi:10.1016/j.atmosenv.2004.01.051, 2004.

Clegg, S. L., Brimblecombe, P., and Wexler, A. S.: Thermodynamic model of the system $H^+ - NH_4^+ - Na^+ - SO_4^{2-} NO_3^- - Cl^- - H_2O$ at 298.15 K, J. Phys. Chem. A, 102, 2155–2171, doi:10.1021/Jp973043j, 1998.

Cruz, C. N. and Pandis, S. N.: Deliquescence and hygroscopic growth of mixed inorganic–organic atmospheric aerosol, Environ. Sci. Technol., 34, 4313–4319, doi:10.1021/Es9907109, 2000.

Dinar, E., Taraniuk, I., Graber, E. R., Katsman, S., Moise, T., Anttila, T., Mentel, T. F., and Rudich, Y.: Cloud Condensation Nuclei properties of model and atmospheric HULIS, Atmos. Chem. Phys., 6, 2465–2482, doi:10.5194/acp-6-2465-2006, 2006.

Dusek, U., Frank, G. P., Massling, A., Zeromskiene, K., Iinuma, Y., Schmid, O., Helas, G., Hennig, T., Wiedensohler, A., and Andreae, M. O.: Water uptake by biomass burning aerosol at sub- and supersaturated conditions: closure studies and implications for the role of organics, Atmos. Chem. Phys., 11, 9519–9532, doi:10.5194/acp-11-9519-2011, 2011.

ACPD
15, 17317–17365, 2015

Ekström, S., Nozière, B., and Hansson, H.-C.: The Cloud Condensation Nuclei (CCN) properties of 2-methyltetrols and C3-C6 polyols from osmolality and surface tension measurements, Atmos. Chem. Phys., 9, 973–980, doi:10.5194/acp-9-973-2009, 2009.

Facchini, M. C., Mircea, M., Fuzzi, S., and Charlson, R. J.: Cloud albedo enhancement by surface-active organic solutes in growing droplets, Nature, 401, 257–259, doi:10.1038/45758, 1999.

Frossard, A. A., Shaw, P. M., Russell, L. M., Kroll, J. H., Canagaratna, M. R., Worsnop, D. R., Quinn, P. K., and Bates, T. S.: Springtime Arctic haze contributions of submicron organic particles from European and Asian combustion sources, J. Geophys. Res.-Atmos., 116, D05205, doi:10.1029/2010jd015178, 2011.

Froyd, K. D., Murphy, S. M., Murphy, D. M., de Gouw, J. A., Eddingsaas, N. C., and Wennberg, P. O.: Contribution of isoprene-derived organosulfates to free tropospheric aerosol mass, P. Natl. Acad. Sci. USA, 107, 21360–21365, doi:10.1073/pnas.1012561107, 2010.

Good, N., Topping, D. O., Allan, J. D., Flynn, M., Fuentes, E., Irwin, M., Williams, P. I., Coe, H., and McFiggans, G.: Consistency between parameterisations of aerosol hygroscopicity and CCN activity during the RHaMBLe discovery cruise, Atmos. Chem. Phys., 10, 3189–3203, doi:10.5194/acp-10-3189-2010, 2010.

Gysel, M., Crosier, J., Topping, D. O., Whitehead, J. D., Bower, K. N., Cubison, M. J., Williams, P. I., Flynn, M. J., McFiggans, G. B., and Coe, H.: Closure study between chemical composition and hygroscopic growth of aerosol particles during TORCH2, Atmos. Chem. Phys., 7, 6131–6144, doi:10.5194/acp-7-6131-2007, 2007.

Gysel, M., McFiggans, G. B., and Coe, H.: Inversion of tandem differential mobility analyser (TDMA) measurements, J. Aerosol Sci., 40, 134–151, doi:10.1016/j.jaerosci.2008.07.013, 2009.

Hallquist, M., Wenger, J. C., Baltensperger, U., Rudich, Y., Simpson, D., Claeys, M., Dommen, J., Donahue, N. M., George, C., Goldstein, A. H., Hamilton, J. F., Herrmann, H., Hoffmann, T., Iinuma, Y., Jang, M., Jenkin, M. E., Jimenez, J. L., Kiendler-Scharr, A., Maenhaut, W., McFiggans, G., Mentel, Th. F., Monod, A., Prévôt, A. S. H., Seinfeld, J. H., Surratt, J. D., Szmigielski, R., and Wildt, J.: The formation, properties and impact of secondary organic aerosol: current and emerging issues, Atmos. Chem. Phys., 9, 5155–5236, doi:10.5194/acp-9-5155-2009, 2009.

ACPD
15, 17317–17365, 2015

Hämeri, K., Charlson, R., and Hansson, H. C.: Hygroscopic properties of mixed ammonium sulfate and carboxylic acids particles, Aiche. J., 48, 1309–1316, doi:10.1002/aic.690480617, 2002.

Hansen, A. M. K., Kristensen, K., Nguyen, Q. T., Zare, A., Cozzi, F., Nøjgaard, J. K., Skov, H., Brandt, J., Christensen, J. H., Ström, J., Tunved, P., Krejci, R., and Glasius, M.: Organosulfates and organic acids in Arctic aerosols: speciation, annual variation and concentration levels, Atmos. Chem. Phys., 14, 7807–7823, doi:10.5194/acp-14-7807-2014, 2014.

Henning, S., Ziese, M., Kiselev, A., Saathoff, H., Möhler, O., Mentel, T. F., Buchholz, A., Spindler, C., Michaud, V., Monier, M., Sellegri, K., and Stratmann, F.: Hygroscopic growth and droplet activation of soot particles: uncoated, succinic or sulfuric acid coated, Atmos. Chem. Phys., 12, 4525–4537, doi:10.5194/acp-12-4525-2012, 2012.

Herich, H., Tritscher, T., Wiacek, A., Gysel, M., Weingartner, E., Lohmann, U., Baltensperger, U., and Cziczo, D. J.: Water uptake of clay and desert dust aerosol particles at sub- and supersaturated water vapor conditions, Phys. Chem. Chem. Phys., 11, 7804–7809, doi:10.1039/b901585j, 2009.

Hersey, S. P., Craven, J. S., Metcalf, A. R., Lin, J., Lathem, T., Suski, K. J., Cahill, J. F., Duong, H. T., Sorooshian, A., Jonsson, H. H., Shiraiwa, M., Zuend, A., Nenes, A., Prather, K. A., Flagan, R. C., and Seinfeld, J. H.: Composition and hygroscopicity of the Los Angeles Aerosol: CalNex, J. Geophys. Res.-Atmos., 118, 3016–3036, doi:10.1002/Jgrd.50307, 2013.

Holmgren, H., Sellegri, K., Hervo, M., Rose, C., Freney, E., Villani, P., and Laj, P.: Hygroscopic properties and mixing state of aerosol measured at the high-altitude site Puy de Dôme (1465 m a.s.l.), France, Atmos. Chem. Phys., 14, 9537–9554, doi:10.5194/acp-14-9537-2014, 2014.

Hong, J., Häkkinen, S. A. K., Paramonov, M., Äijälä, M., Hakala, J., Nieminen, T., Mikkilä, J., Prisle, N. L., Kulmala, M., Riipinen, I., Bilde, M., Kerminen, V.-M., and Petäjä, T.: Hygroscopicity, CCN and volatility properties of submicron atmospheric aerosol in a boreal forest environment during the summer of 2010, Atmos. Chem. Phys., 14, 4733–4748, doi:10.5194/acp-14-4733-2014, 2014.

Iinuma, Y., Müller, C., Berndt, T., Böge, O., Claeys, M., and Herrmann, H.: Evidence for the existence of organosulfates from beta-pinene ozonolysis in ambient secondary organic aerosol, Environ. Sci. Technol., 41, 6678–6683, doi:10.1021/Es070938t, 2007.

ACPD
15, 17317–17365, 2015

IPCC: Summary for Policymakers, Cambridge University Press, Cambridge, UK, New York, NY, USA, 2013.
Kiss, G., Tombacz, E., and Hansson, H. C.: Surface tension effects of humic-like substances in the aqueous extract of tropospheric fine aerosol, J. Atmos. Chem., 50, 279–294, doi:10.1007/s10874-005-5079-5, 2005.
Koehler, K. A., Kreidenweis, S. M., DeMott, P. J., Prenni, A. J., Carrico, C. M., Ervens, B., and Feingold, G.: Water activity and activation diameters from hygroscopicity data – Part II: Application to organic species, Atmos. Chem. Phys., 6, 795–809, doi:10.5194/acp-6-795-2006, 2006.
Kristensen, K. and Glasius, M.: Organosulfates and oxidation products from biogenic hydrocarbons in fine aerosols from a forest in North West Europe during spring, Atmos. Environ., 45, 4546–4556, doi:10.1016/j.atmosenv.2011.05.063, 2011.
Kristensen, T. B., Prisle, N. L., and Bilde, M.: Cloud droplet activation of mixed model HULIS and NaCl particles: experimental results and kappa-Kohler theory, Atmos. Res., 137, 167–175, doi:10.1016/j.atmosres.2013.09.017, 2014.
Lee, J. Y. and Hildemann, L. M.: Surface tension of solutions containing dicarboxylic acids with ammonium sulfate, D-glucose, or humic acid, J. Aerosol Sci., 64, 94–102, doi:10.1016/j.jaerosci.2013.06.004, 2013.
Lin, P., Huang, X. F., He, L. Y., and Yu, J. Z.: Abundance and size distribution of HULIS in ambient aerosols at a rural site in South China, J. Aerosol Sci., 41, 74–87, doi:10.1016/j.jaerosci.2009.09.001, 2010.
Lin, Y. H., Zhang, Z. F., Docherty, K. S., Zhang, H. F., Budisulistiorini, S. H., Rubitschun, C. L., Shaw, S. L., Knipping, E. M., Edgerton, E. S., Kleindienst, T. E., Gold, A., and Surratt, J. D.: Isoprene epoxydiols as precursors to secondary organic aerosol formation: acid-catalyzed reactive uptake studies with authentic compounds, Environ. Sci. Technol., 46, 250–258, doi:10.1021/Es202554c, 2012.
Massling, A., Stock, M., Wehner, B., Wu, Z. J., Hu, M., Bruggemann, E., Gnauk, T., Herrmann, H., and Wiedensohler, A.: Size segregated water uptake of the urban submicrometer aerosol in Beijing, Atmos. Environ., 43, 1578–1589, doi:10.1016/j.atmosenv.2008.06.003, 2009.
Massoli, P., Lambe, A. T., Ahern, A. T., Williams, L. R., Ehn, M., Mikkilä, J., Canagaratna, M. R., Brune, W. H., Onasch, T. B., Jayne, J. T., Petäjä, T., Kulmala, M., Laaksonen, A., Kolb, C. E., Davidovits, P., and Worsnop, D. R.: Relationship between aerosol oxidation level and hy-

ACPD
15, 17317–17365, 2015

groscopic properties of laboratory generated secondary organic aerosol (SOA) particles, Geophys. Res. Lett., 37, L24801, doi:10.1029/2010gl045258, 2010.
Matubayasi, N.: Surface Tension and Related Thermodynamic Quantities of Aqueous Electrolyte Solutions, CRC Press, Boca Raton, Florida, 2013.
Mochida, M., Kitamori, Y., Kawamura, K., Nojiri, Y., and Suzuki, K.: Fatty acids in the marine atmosphere: factors governing their concentrations and evaluation of organic films on sea-salt particles, J. Geophys. Res.-Atmos., 107, 4325, doi:10.1029/2001jd001278, 2002.
Nguyen, Q. T., Christensen, M. K., Cozzi, F., Zare, A., Hansen, A. M. K., Kristensen, K., Tulinius, T. E., Madsen, H. H., Christensen, J. H., Brandt, J., Massling, A., Nøjgaard, J. K., and Glasius, M.: Understanding the anthropogenic influence on formation of biogenic secondary organic aerosols in Denmark via analysis of organosulfates and related oxidation products, Atmos. Chem. Phys., 14, 8961–8981, doi:10.5194/acp-14-8961-2014, 2014.
Pajunoja, A., Lambe, A. T., Hakala, J., Rastak, N., Cummings, M. J., Brogan, J. F., Hao, L., Paramonov, M., Hong, J., Prisle, N. L., Malila, J., Romakkaniemi, S., Lehtinen, K. E. J., Laaksonen, A., Kulmala, M., Massoli, P., Onasch, T. B., Donahue, N. M., Riipinen, I., Davidovits, P., Worsnop, D. R., Petäjä, T., and Virtanen, A.: Adsorptive uptake of water by semisolid secondary organic aerosols, Geophys. Res. Lett., 42, 3063–3068, doi:10.1002/2015gl063142, 2015.
Paramonov, M., Aalto, P. P., Asmi, A., Prisle, N., Kerminen, V.-M., Kulmala, M., and Petäjä, T.: The analysis of size-segregated cloud condensation nuclei counter (CCNC) data and its implications for cloud droplet activation, Atmos. Chem. Phys., 13, 10285–10301, doi:10.5194/acp-13-10285-2013, 2013.
Petters, M. D. and Kreidenweis, S. M.: A single parameter representation of hygroscopic growth and cloud condensation nucleus activity, Atmos. Chem. Phys., 7, 1961–1971, doi:10.5194/acp-7-1961-2007, 2007.
Petters, M. D., Wex, H., Carrico, C. M., Hallbauer, E., Massling, A., McMeeking, G. R., Poulain, L., Wu, Z., Kreidenweis, S. M., and Stratmann, F.: Towards closing the gap between hygroscopic growth and activation for secondary organic aerosol – Part 2: Theoretical approaches, Atmos. Chem. Phys., 9, 3999–4009, doi:10.5194/acp-9-3999-2009, 2009.
Prenni, A. J., Petters, M. D., Kreidenweis, S. M., DeMott, P. J., and Ziemann, P. J.: Cloud droplet activation of secondary organic aerosol, J. Geophys. Res.-Atmos., 112, D10223, doi:10.1029/2006jd007963, 2007.

ACPD
15, 17317–17365, 2015

Prisle, N. L.: Cloud Condensation Nuclei Properties of Organic Aerosol Particles: Effects of Acid Dissociation and Surfactant Partitioning, M.Sc. thesis, Department of Chemistry, Faculty of Science, University of Copenhagen, Copenhagen, Denmark, 2006.
Prisle, N. L., Raatikainen, T., Sorjamaa, R., Svenningsson, B., Laaksonen, A., and Bilde, M.: Surfactant partitioning in cloud droplet activation: a study of C8, C10, C12 and C14 normal fatty acid sodium salts, Tellus B, 60, 416–431, doi:10.1111/j.1600-0889.2008.00352.x, 2008.
Prisle, N. L., Engelhart, G. J., Bilde, M., and Donahue, N. M.: Humidity influence on gas-particle phase partitioning of alpha-pinene + O-3 secondary organic aerosol, Geophys. Res. Lett., 37, L01802, doi:10.1029/2009gl041402, 2010a.
Prisle, N. L., Raatikainen, T., Laaksonen, A., and Bilde, M.: Surfactants in cloud droplet activation: mixed organic-inorganic particles, Atmos. Chem. Phys., 10, 5663–5683, doi:10.5194/acp-10-5663-2010, 2010b.
Prisle, N. L., Dal Maso, M., and Kokkola, H.: A simple representation of surface active organic aerosol in cloud droplet formation, Atmos. Chem. Phys., 11, 4073–4083, doi:10.5194/acp-11-4073-2011, 2011.
Prisle, N. L., Asmi, A., Topping, D., Partanen, A. I., Romakkaniemi, S., Dal Maso, M., Kulmala, M., Laaksonen, A., Lehtinen, K. E. J., McFiggans, G., and Kokkola, H.: Surfactant effects in global simulations of cloud droplet activation, Geophys Res. Lett., 39, L05802, doi:10.1029/2011gl050467, 2012.
Rose, D., Gunthe, S. S., Mikhailov, E., Frank, G. P., Dusek, U., Andreae, M. O., and Pöschl, U.: Calibration and measurement uncertainties of a continuous-flow cloud condensation nuclei counter (DMT-CCNC): CCN activation of ammonium sulfate and sodium chloride aerosol particles in theory and experiment, Atmos. Chem. Phys., 8, 1153–1179, doi:10.5194/acp-8-1153-2008, 2008.
Rose, D., Nowak, A., Achtert, P., Wiedensohler, A., Hu, M., Shao, M., Zhang, Y., Andreae, M. O., and Pöschl, U.: Cloud condensation nuclei in polluted air and biomass burning smoke near the mega-city Guangzhou, China – Part 1: Size-resolved measurements and implications for the modeling of aerosol particle hygroscopicity and CCN activity, Atmos. Chem. Phys., 10, 3365–3383, doi:10.5194/acp-10-3365-2010, 2010.
Seinfeld, J. H. and Pandis, S. N.: Atmospheric Chemistry and Physics: from Air Pollution to Climate Change, Wiley, Hoboken, New Jersey, 2006.
Sjogren, S., Gysel, M., Weingartner, E., Alfarra, M. R., Duplissy, J., Cozic, J., Crosier, J., Coe, H., and Baltensperger, U.: Hygroscopicity of the submicrometer aerosol at the high-

ACPD
15, 17317–17365, 2015

alpine site Jungfraujoch, 3580 m a.s.l., Switzerland, Atmos. Chem. Phys., 8, 5715–5729, doi:10.5194/acp-8-5715-2008, 2008.
Song, J. Z., He, L. L., Peng, P. A., Zhao, J. P., and Ma, S. X.: Chemical and Isotopic Composition of Humic-Like Substances (HULIS) in ambient aerosols in Guangzhou, South China, Aerosol Sci. Tech., 46, 533–546, doi:10.1080/02786826.2011.645956, 2012.
Stokes, R. H. and Robinson, R. A.: Interactions in aqueous nonelectrolyte solutions, I. Solute-solvent equilibria, J. Phys. Chem.-US, 70, 2126–2131, doi:10.1021/J100879a010, 1966.
Suda, S. R., Petters, M. D., Yeh, G. K., Strollo, C., Matsunaga, A., Faulhaber, A., Ziemann, P. J., Prenni, A. J., Carrico, C. M., Sullivan, R. C., and Kreidenweis, S. M.: Influence of functional groups on organic aerosol cloud condensation nucleus activity, Environ. Sci. Technol., 48, 10182–10190, doi:10.1021/Es502147y, 2014.
Surratt, J. D., Kroll, J. H., Kleindienst, T. E., Edney, E. O., Claeys, M., Sorooshian, A., Ng, N. L., Offenberg, J. H., Lewandowski, M., Jaoui, M., Flagan, R. C., and Seinfeld, J. H.: Evidence for organosulfates in secondary organic aerosol, Environ. Sci. Technol., 41, 517–527, doi:10.1021/Es062081q, 2007.
Surratt, J. D., Gómez-González, Y., Chan, A. W. H., Vermeylen, R., Shahgholi, M., Kleindienst, T. E., Edney, E. O., Offenberg, J. H., Lewandowski, M., Jaoui, M., Maenhaut, W., Claeys, M., Flagan, R. C., and Seinfeld, J. H.: Organosulfate formation in biogenic secondary organic aerosol, J. Phys. Chem. A, 112, 8345–8378, doi:10.1021/Jp802310p, 2008.
Swietlicki, E., Hansson, H. C., Hämeri, K., Svenningsson, B., Massling, A., McFiggans, G., McMurry, P. H., Petäjä, T., Tunved, P., Gysel, M., Topping, D., Weingartner, E., Baltensperger, U., Rissler, J., Wiedensohler, A., and Kulmala, M.: Hygroscopic properties of submicrometer atmospheric aerosol particles measured with H-TDMA instruments in various environments – a review, Tellus B, 60, 432–469, doi:10.1111/j.1600-0889.2008.00350.x, 2008.
Wex, H., McFiggans, G., Henning, S., and Stratmann, F.: Influence of the external mixing state of atmospheric aerosol on derived CCN number concentrations, Geophys. Res. Lett., 37, L10805, doi:10.1029/2010gl043337, 2010.
Zardini, A. A., Sjogren, S., Marcolli, C., Krieger, U. K., Gysel, M., Weingartner, E., Baltensperger, U., and Peter, T.: A combined particle trap/HTDMA hygroscopicity study of mixed inorganic/organic aerosol particles, Atmos. Chem. Phys., 8, 5589–5601, doi:10.5194/acp-8-5589-2008, 2008.

ACPD
15, 17317–17365, 2015

Table 1. Composition and concentration range of the solutions used for surface tension measurements.

Composition [% *wt*/*wt*]		# solutions	Concentration range [mol L^{-1}]	
L-OS 250	AS		L-OS 250	AS
100	0	12	0.0001–0.24	–
80	20	10	0.0001–0.20	0.00005–0.10
50	50	9	0.0001–0.10	0.0002–0.20
20	80	9	0.0001–0.05	0.0007–0.37
10	90	9	0.0001–0.05	0.0017–0.85
5	95	9	0.0001–0.07	0.0035–2.7

ACPD
15, 17317–17365, 2015

Table 2. Solutions of L-OS 250, AS and mixtures hereof for measurement of hygroscopic growth factor and CCN activation.

Composition [% wt/wt]		Total solute concentration [g L^{-1}]
L-OS 250	AS	
100	0	0.21
90	10	0.21
80	20	0.20
50	50	0.22
20	80	0.19
0	100	0.25

ACPD
15, 17317–17365, 2015

Table 3. Mean, minimum and maximum values of the hygroscopicity parameter, κ, obtained from the CCN measurements, as well as standard deviations.

	κ_{CCN}			
	Mean	SD	Minimum	Maximum
L-OS 250	0.120	0.017	0.095	0.145
L-OS 250 (10 % w/w AS)	0.207	0.013	0.182	0.229
L-OS 250 (20 % w/w AS)	0.510	0.022	0.486	0.566
L-OS 250 (50 % w/w AS)	0.519	0.028	0.496	0.589
L-OS 250 (80 % w/w AS)	0.532	0.027	0.501	0.597
AS	0.538	0.026	0.509	0.594

ACPD
15, 17317–17365, 2015

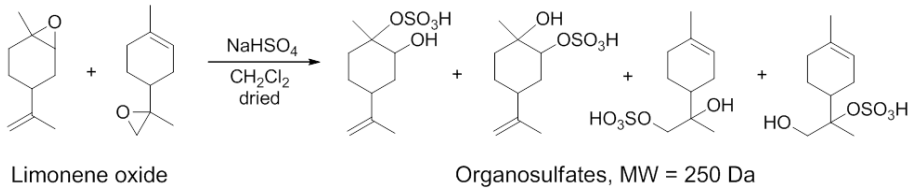

Figure 1. Synthesis of limonene-derived organosulfates with a molecular mass of 250 Da (L-OS 250) by ring opening of limonene epoxides with sodium hydrogen sulfate. The reaction is based on Cavdar and Saracoglu (2009).

ACPD
15, 17317–17365, 2015

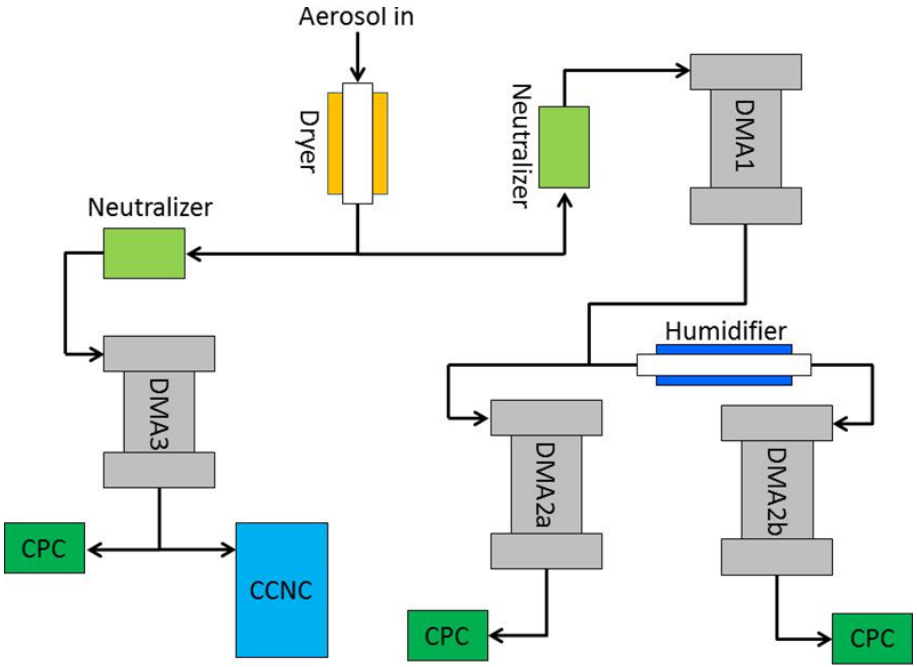

Figure 2. Schematic illustration of the experimental set-up for the dual H-TDMA and CCN measurements.

ACPD
15, 17317–17365, 2015

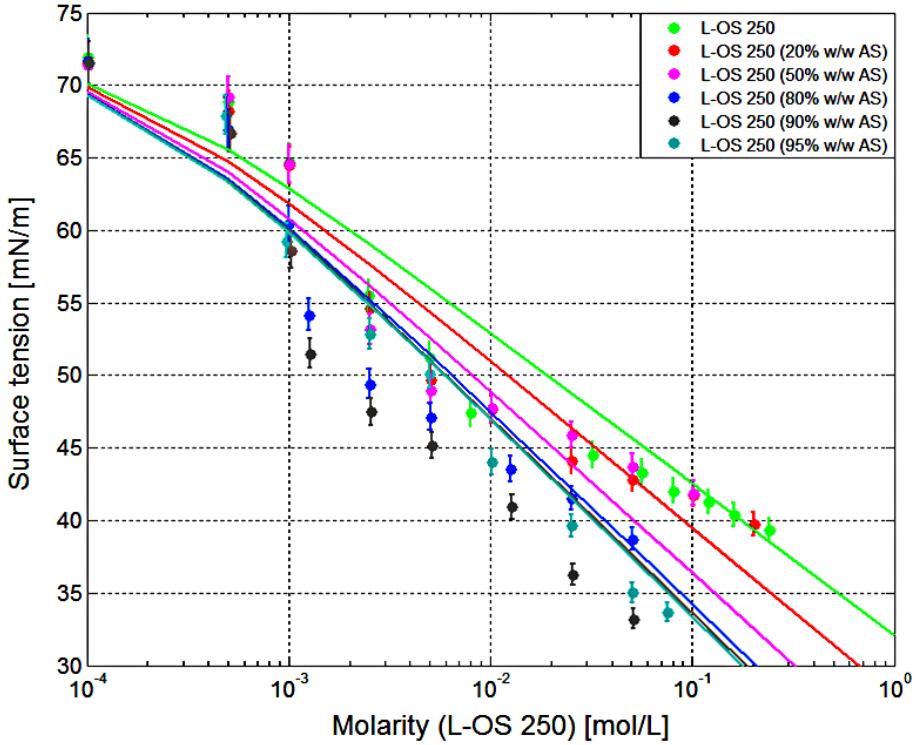

Figure 3. Surface tension as a function of the concentration of limonene organosulfate (L-OS 250) for six mixtures of L-OS 250 and ammonium sulphate (AS). Note that the data is plotted in semi-log space. Lines represent parametrisation curves and error bars show the 2 % instrumental uncertainty.

ACPD
15, 17317–17365, 2015

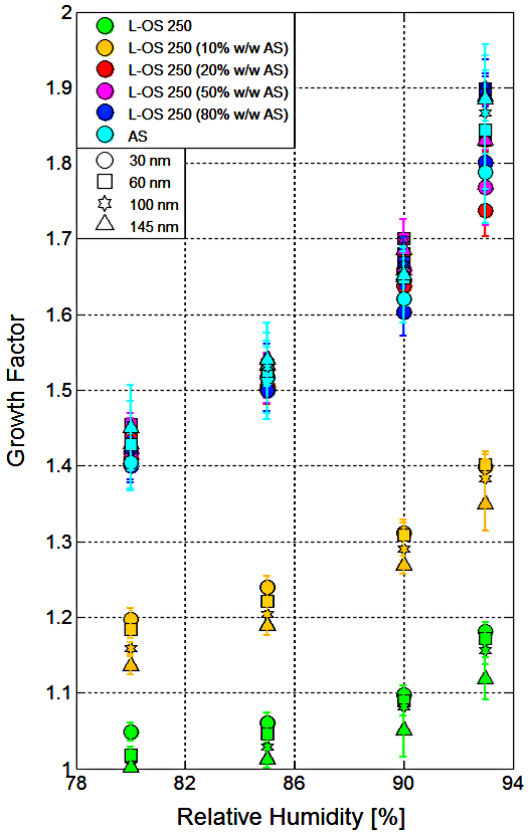

Figure 4. Hygroscopic growth factor (HGF) as a function of relative humidity (RH) for particles of pure L-OS 250, pure AS and mixtures hereof. Growth factor is given for four dry particle diameters of each chemical composition. Each dot represents the mean HGF obtained from 4 to 6 measurements, and the error bars express ± two standard deviations as described in Sect. 2.3.

ACPD
15, 17317–17365, 2015

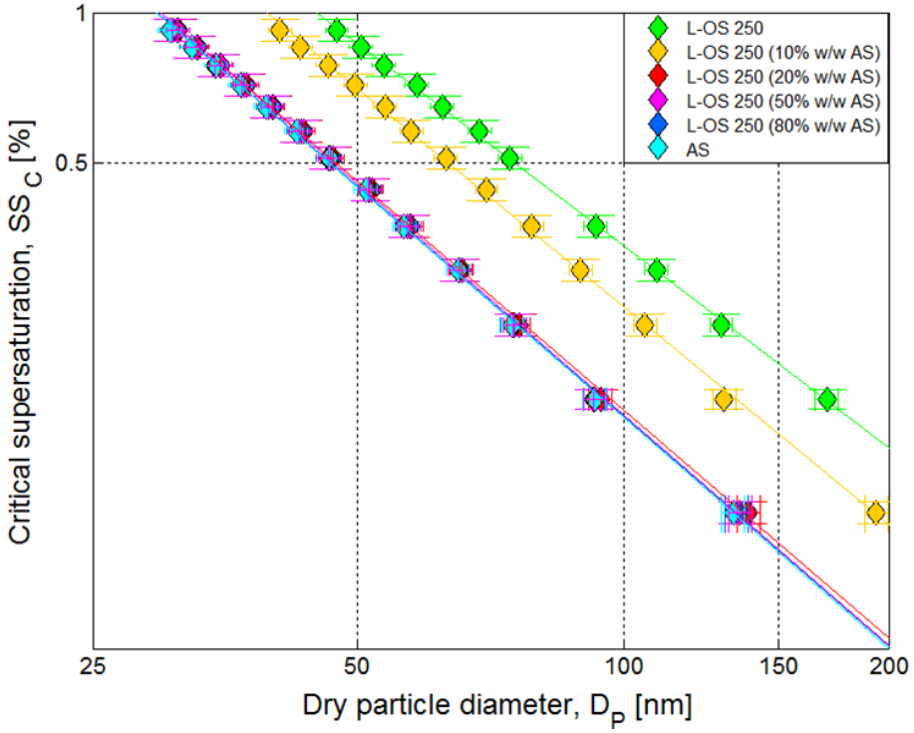

Figure 5. Critical supersaturation (SSc) as function of dry particle diameter for the six investigated particle compositions. The curves follow the Köhler slope of approximately −3/2. Error bars represent the uncertainty on the particle dry size (x axis) and SSc (y axis). Note that the data is plotted in log-log space.

ACPD
15, 17317–17365, 2015

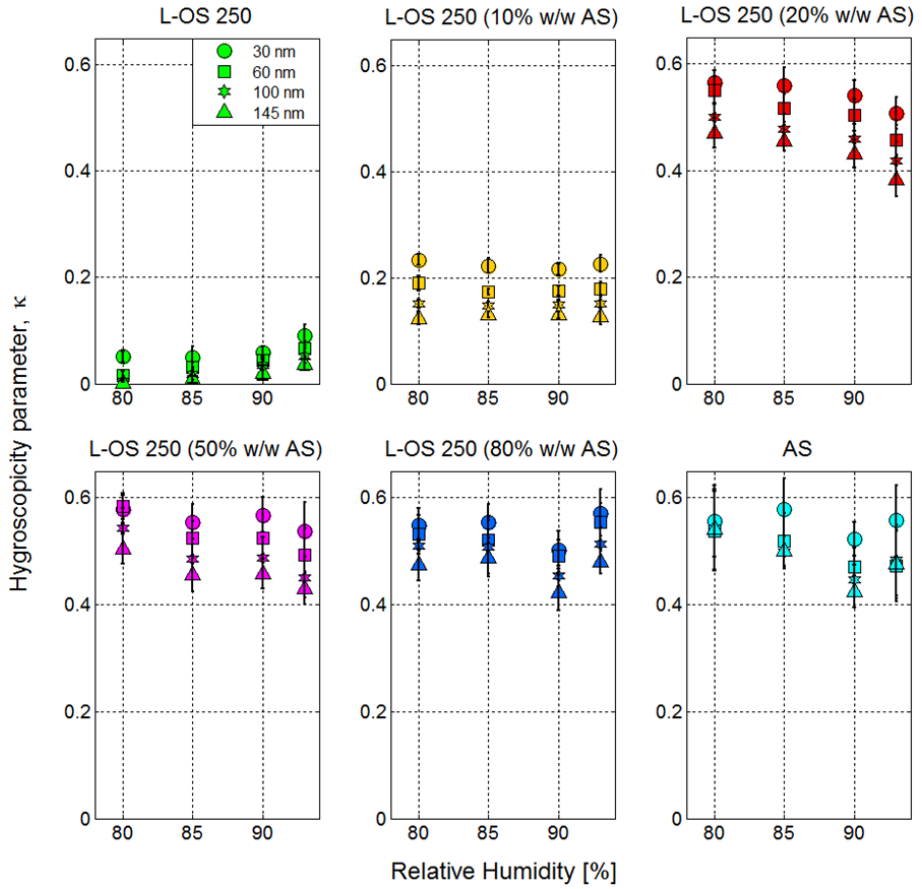

Figure 6. Hygroscopicity parameter, κ, obtained from the H-TDMA measurements, as a function of RH for the six mixtures of L-OS 250 and AS. Error bars represent ± two standard deviations on κ as described in Sect. 2.3.1.

ACPD
15, 17317–17365, 2015

Hygroscopic properties of limonene organosulfate

A. M. K. Hansen et al.

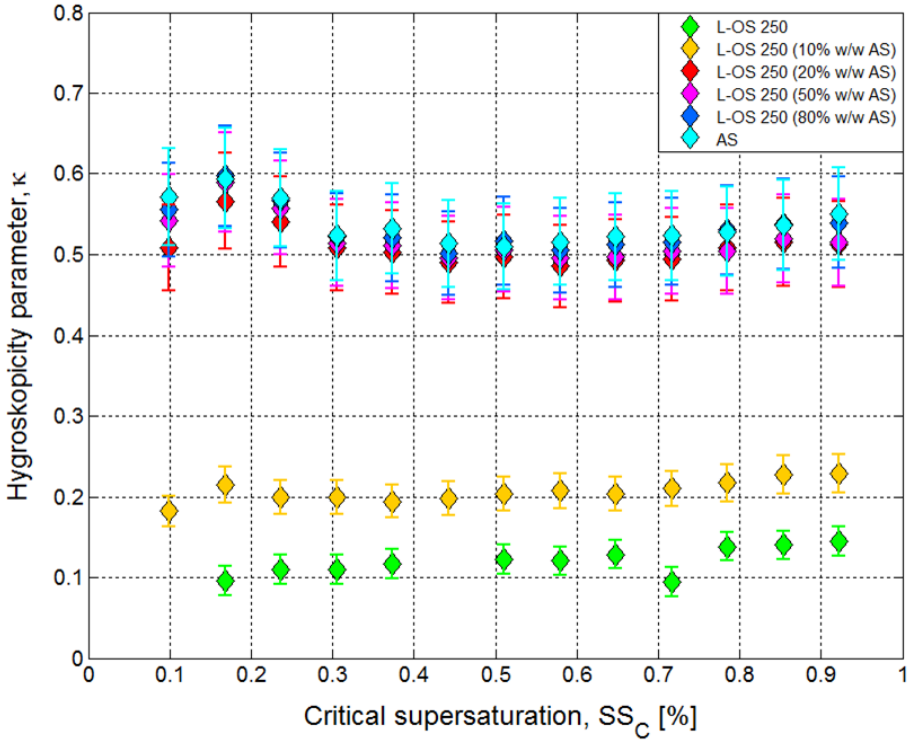

Figure 7. Hygroscopicity parameter, κ, derived from the CCN measurements, as a function of SSc for six mixtures of L-OS 250 and AS. Error bars represent an estimated uncertainty of 10 % on κ and uncertainty on the SSc is estimated to be 5 %/% as described in Sect. 2.3.1.

ACPD
15, 17317–17365, 2015

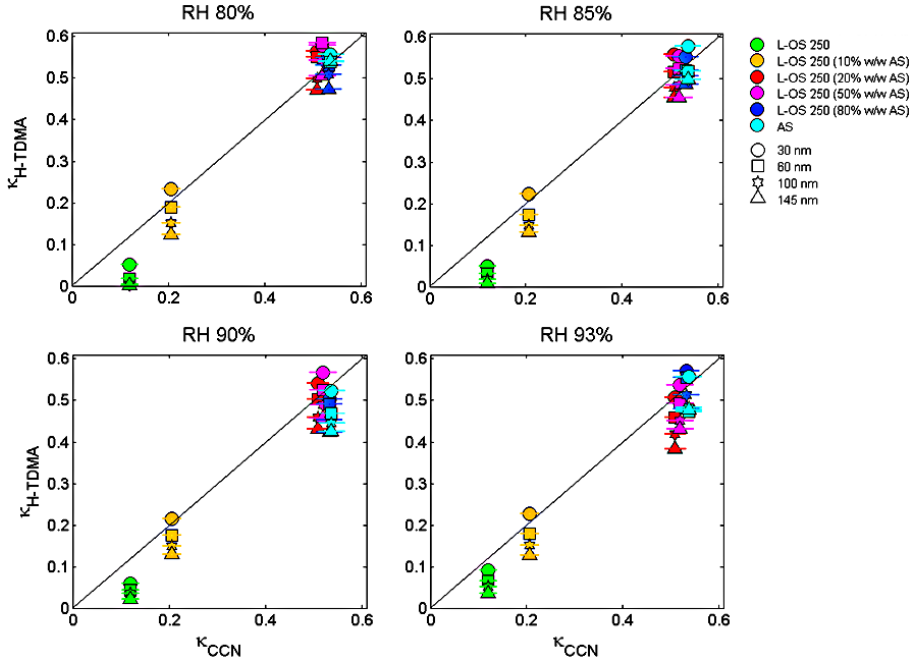

Figure 8. Hygroscopicity parameter, κ, derived from the H-TDMA measurements, as a function of κ obtained from the CCN measurements, for six mixtures of L-OS 250 and AS. A mean κ-values for each composition was found for the CCN-derived κ and error bars denote the uncertainty as explained in Sect. 2.3.1.

ACPD
15, 17317–17365, 2015

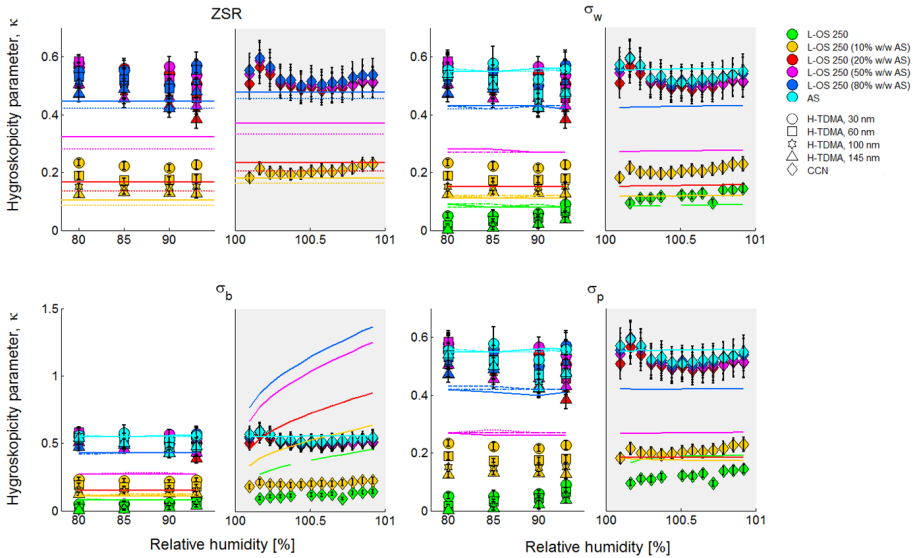

Figure 9. Measured and modelled hygroscopicity parameter, κ, as a function of RH for six mixtures of L-OS 250 and AS. Markers represent the measured values of κ and lines represent the modelled values of κ. The light grey area denotes humidity in the supersaturated range (CCN) and the white area denotes humidity in the subsaturated range (H-TDMA). For subfigure ZSR the solid lines represent additive κ calculated using a density of 1.176 g cm^{-3} for L-OS 250 whereas a density of 1.7 g cm^{-3} is represented with the dotted lines. For subfigure σ_p, the subsaturated range, the solid line is modelledκ for 30 nm particles, the dash-dotted line is modelled κ for 60 nm particles, the dotted line is modelled κ for 100 nm particles and the dashed line is modelled κ for 145 nm particles. Error bars represent the uncertainty on the κ-values obtained from the measurements (±10 % on κ_{CCN} and ± two standard deviation on $\kappa_{H\text{-}TDMA}$). Please note that the y axis in subfigure σ_b is different form the other subfigures.

ACPD
15, 17317–17365, 2015

Hygroscopic properties of limonene organosulfate

A. M. K. Hansen et al.

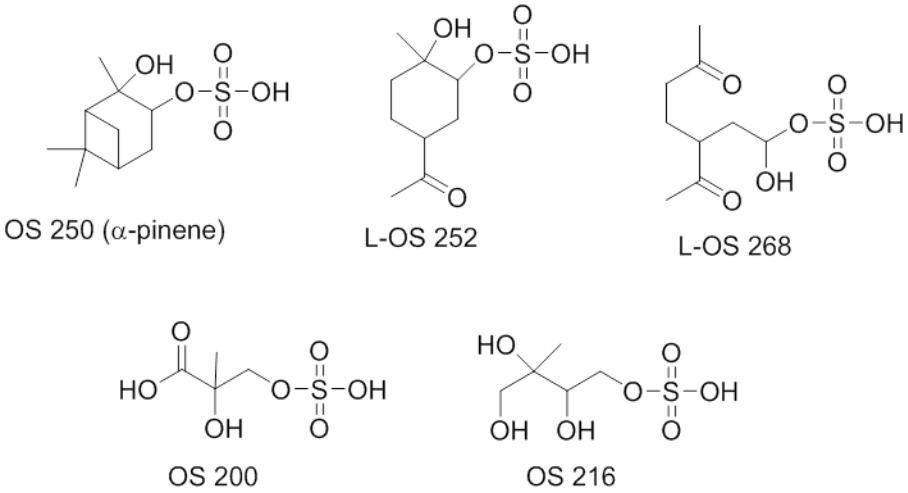

Figure 10. Selected organosulfates derived from monoterpenes and isoprene (Surratt et al., 2007, 2008). Note that isomers are possible for the given structures.

ACPD
15, 17317–17365, 2015